Dynamic Modeling and Identification of Par4, A Very High Speed Parallel Manipulator

Vincent NABAT

Fundación FATRONIK

Elgoibar (Gipuzcoa) - Spain

nabat@lirmm.fr

Olivier COMPANY, François PIERROT, and Philippe POIGNET

LIRMM

UMR 5506 CNRS - University of Montpellier

Montpellier - France

<company, pierrot, poignet> @lirmm.fr

Abstract **– This paper introduces the dynamic modeling and the identification of Par4, a four-degree-of-freedom parallel manipulator producing Schonflies motions (three translations and one rotation about a fixed axis). First of all, this paper presents how this robot is developed with the goal of reaching very high speed. Indeed, it is an evolution of Delta, H4 and I4 robots architectures: it keeps their advantages while overcoming their drawbacks. Experimentations done with the prototype prove that the robot is able to reach very high accelerations (15 G) and to perform an Adept cycle in 0.25 s. In order to improve its dynamic accuracy, a dynamic control could be necessary. Thus, this paper presents the dynamic modeling of the manipulator using a simplified Newton-Euler approach. The originality of this computation is to model the traveling as two separated parts and to determine the dynamic effects applied on each of them. Finally, since a dynamic control requires a good evaluation of dynamic parameters, an experimental dynamic identification is presented.**

Index Terms – Dynamic Modeling, Dynamic Identification, Schoenflies Motion, PKM, Articulated traveling plate

I. Introduction

A new trend in the researches on parallel robotics is the development of lower mobility manipulators. Indeed, a lot of applications do not need six degrees of freedom (*dof*). A classification proposed by Brogardh [1] gives the necessary number of *dof* for different industrial applications. He shows that applications such as pick-and-place, assembly, cutting, measurement, etc. just need from three up to five *dof*. This paper focuses on 4 *dof* manipulators and particularly on 3T1R (3 translations – 1 rotation) architectures.

SCARA robots (see Fig. 1a) were the first manipulators developed to produce these movements, also named Schoenflies motion [2]. These robots can reach good performances, but their serial architecture limits their velocities and accelerations. Indeed, this type of mechanism involves high moving masses which are not suitable for high dynamics. This problem can be overcome using parallel architectures first introduced by Gough [3] and Stewart [4]. The most famous 3T1R parallel mechanism was developed by Clavel [5] (see Fig. 1b): the Delta is composed of three closed kinematic chains linking the traveling plate to the frame. Each chain is composed by an arm and a spatial parallelogram (the forearm).

(a) SCARA robot architecture (b) Delta robot architecture

Fig. 1 Serial and Parallel 3T1R manipulators

However, this architecture is able to produce three translations and the rotational motion is obtained using a central "telescopic" leg built with universal and prismatic joints. Other architecture close to Delta, but using linear actuators is the Orthoglide [6]. Its particularity is to be isotropic at the center of its workspace.

Other lower mobility mechanisms were developed in order to produce Schonflies motions. For example, the machine tool HITA STT has been proposed for reaching high tilting angle [7]. The particularity of this architecture is to use additional parts in the traveling plate in order to amplify the rotational motion. Schonflies motion generators have also been proposed by Angeles, such as Gross Manipulator [8] and SMG [9]. We can also mention Kanuk and Manta robots [10]. The first one is a fully parallel robot, but has a short rotational motion; whereas the second one is a hybrid architecture having unlimited rotation. Finally, H4 [11] and I4 [12] are 3T1R parallel manipulators using the concept of articulated traveling plate. The rotational movement is obtained using an internal mobility on the traveling plate, and an amplification or transforming device gives the desired range of rotational motion.

This paper presents a new architecture based on H4 and I4 architecture. This manipulator, named Par4, is an evolution of these mechanisms, and has been developed with the wish of reaching high speeds and accelerations. The paper presents experimental results showing that Par4 is able to reach an acceleration of 15 G. These performances have been obtained using a simple PI controller, but in order to go further, a dynamic control is planed to be implemented. The first step of the integration of such a control is to compute the inverse dynamic modeling of the robot. That is why this paper is focused on the dynamic modeling and the experimental dynamic identification.

II. Description Of Par4

A. Description of the prototype

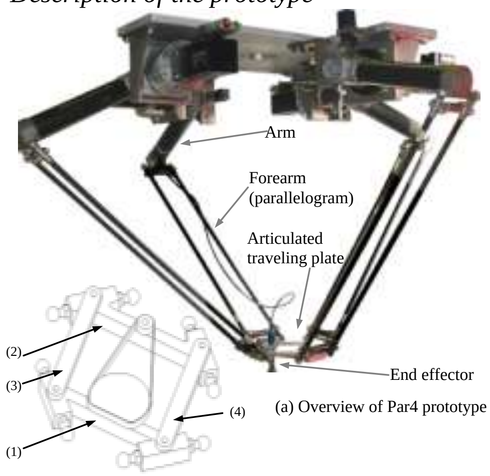

(a) Overview of Par4 prototype

(b) Articulated traveling plate

Fig. 2 Par4 prototype

Par4 is a parallel manipulator composed of four closed kinematic chains and an articulated traveling plate. The kinematic chains are similar to the Delta, H4 and I4 ones. They are composed of an arm and a spatial parallelogram (forearm) linked with spherical joints. The traveling plate is composed of four parts: two main parts (1,2) linked by two bars (3,4) with revolute joints (see Fig. 2). Thus, its shape is a planar parallelogram and the internal mobility of this traveling plate is a circular translation produced by a PI joint [13].

The prototype is built using arms and forearms made of carbon fiber (obtained from ABB Robotics, as spare parts of the commercial FlexPicker robot). The traveling plate is made of aluminum in order to decrease the moving masses.

In addition, the “natural” range of the rotational operational motion is $-\pi/4\,;\,\pi/4$. That is why an amplification system has to be added on the traveling plate in order to make a complete turn: $-\pi\,;\,\pi$. Several options are available for this amplification such as gears or belt/pulleys. The prototype has been built using belt/pulleys system, with the first pulley fixed on one half traveling plate, and the second one is linked with a revolute joint to the second half traveling plate (see Fig. 2b).

From a kinematic and geometric point of view, the modeling of Par4 can be assimilated to H4. These models are presented in [11].

This robot has been developed with the goal of taking advantages of the existing architectures, such as Delta, H4 and I4, and using the feedback of these developments to build a manipulator having the best possible performances.

B. Evolution of Par4 compared to Delta, H4 and I4

The key point of the study was to develop a robot able to reach very high dynamics, and having a homogenous behavior in the whole workspace. All these characteristics cannot be achieved at the same time neither by Delta, nor H4, nor I4.

1) Delta robot

The main weak point of Delta robot is the central telescopic leg providing the rotational motion. This **R**UPUR (R: revolute, U: universal, P: prismatic joints) chain suffers from a short service life, and involves a bad stiffness of the rotation motion.

In order to avoid the central telescopic leg, the concept of articulated traveling plate has been introduced with H4 and I4.

2) H4 robot

The traveling plate of H4 is realized with three parts linked by revolute joints (see Fig. 3a). A complete study of singularities of this robot including the notion of “internal singularities” has been developed in [11] and demonstrates that placing actuators in a symmetrical way, *i.e.* at 90° one relatively to each other involves singular postures. Thus, the robot has to be built using a particular arrangement of motors, whose axes are presented in Fig. 3a with arrows. This non symmetrical arrangement entails a non homogenous behavior in the workspace and a limited stiffness [14] of the robot.

3) I4 robot

The internal mobility of I4 is obtained with a prismatic joint (Fig. 3b). The advantage of this architecture is to authorize a symmetrical arrangement of the actuators. As demonstrated in [12], it is possible to place the actuators at 90° one relatively to each other. However, this architecture is more adapted to machine-tool application than to high speed pick-and-place. Indeed, commercial prismatic joints are not suitable for high speed and high accelerations, and have a short service life under such conditions. This inconvenient is due to the high pressure exerted on the balls of these elements at high acceleration conditions.

4) Par4 robot

Due to its traveling plate having the shape of a planar parallelogram, Par4 has all the advantages of the previous robots, without their drawbacks. Indeed, as presented in § II.A, the traveling plate of this robot is articulated, and is exclusively realized with revolute joints. In addition, a complete study of singularities presented in [15] demonstrates that it is possible to have the same arrangements of the actuators as I4. Thus, this robot is well suited to reach high dynamics and, at the same time, to have a good stiffness and a homogenous behavior in the workspace.

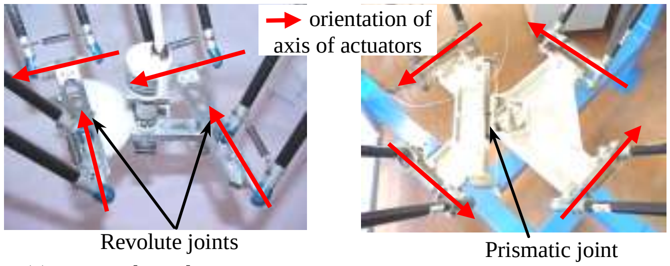

(a) H4 traveling plate (b) I4 traveling plate

Fig. 3 Traveling plate of H4 and I4 and orientation of the axis of actuators

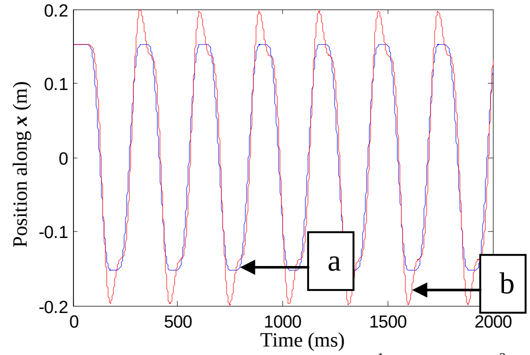

Fig. 4 Evolution of position along $\boldsymbol{x}$ (v =5 m.s^{-1}, a = 150 m.s^{-2})

A prototype has been built, and some experimentations have been carried out. The experimentations show that the theoretical expectations are valid, and prove that this architecture is able to achieve very high performances as described in the next section.

III. Experimental Results

Experimentations have been done with the prototype. The tests have been performed with trajectories called "Adept motions". These trajectories are classical industrial motions used to characterize pick-and-place robots and correspond to a round trip motion. The controller used for these experimentations is a P controller applied on the actuated velocities and a P-I controller on the joint positions.

Fig. 4 shows the desired trajectory (a-plot) and the obtained trajectory (b-plot) for a test performed with a velocity (v) equal to 5 m.s^{-1} and an acceleration (a) equal to 150 m.s^{-2} (~ 15 G). The obtained cycle time, corresponding to a round trip, is 0.25 s.

This test shows that the robot is able to have a good behavior at very high dynamics. However, we can notice that the overshoot is important.

Indeed, the P-I controller is not accurate enough, and the use of a dynamic control, and later, a predictive control [15] should give better results.

In order to implement such control laws, dynamic modeling of the robot is necessary. The following section (§IV) will focus on its derivation. In addition, the quality of this controller requires a good precision of the dynamic parameters. Thus, the estimation of these parameters have to be done, and is presented at § V.

IV. Dynamic Modeling

Khalil developed a method to model the dynamics of parallel robots in [17]. This method permits to model the whole dynamics of the architecture and considers all the parts of all the kinematic chains.

In our case, Par4 is a robot having lightweight parts. Thus, it is possible to make some assumptions leading to a simpler and more time-efficient model. These simplifications will be explained in this section.

This computation will be used, in a future work, to implement dynamic and predictive controllers.

A. *Parameters and simplifications*

Let's first define geometrical and dynamical parameters that have been introduced:

- P_i: center of actuated revolute joints
- A_i: geometrical point situated at the middle of the two centers of spherical joints of forearms on actuated side of forearms
- B_i: geometrical point situated at the middle of the two centers of spherical joints of forearms on traveling plate side of forearms
- θ is the controlled angle in absolute coordinates,
- $\boldsymbol{Q}$, $\dot{\boldsymbol{Q}}$ and $\ddot{\boldsymbol{Q}}$ are the vector of joint positions q_i, velocities $\dot{q}_i$ and acceleration $\ddot{q}_i$
- $\boldsymbol{X}$, $\dot{\boldsymbol{X}}$ and $\ddot{\boldsymbol{X}}$ are the vector of operational positions $x\,y\,z\,\theta\ ^T$, velocities $\left[\dot{x}\,\dot{y}\,\dot{z}\,\dot{\theta}\right]^T$ and acceleration $\left[\ddot{x}\,\ddot{y}\,\ddot{z}\,\ddot{\theta}\right]^T$
- h is the length of the parallelogram of traveling-plate,
- $\boldsymbol{u_i}$ is the unit vector collinear to the axis of actuator,
- i_a: inertia of arms, i_{fa}: inertia of forearms, i_m : inertia of gears and actuator,
- L_i is the length of arms, and l_i is the length of forearms

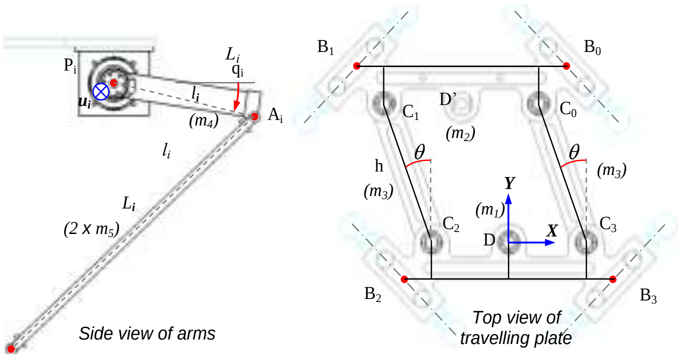

Fig. 5 Parameters used in dynamic modeling

- m_1: mass of first half traveling plate (B_2B_3 side), m_2: mass of second half traveling plate (B_0B_1 side), m_3: mass of rods $\boldsymbol{C_iC_j}$ of the planar parallelogram of the traveling plate, m_4: mass of arms, m_5: mass of forearms (of each rod)
- $\boldsymbol{I_{act}}$: inertia matrix of actuators
- $\boldsymbol{M_1}$: mass matrix of first half traveling plate (B_0B_1 side)
- $\boldsymbol{M_2}$: mass matrix of second half traveling plate (B_2B_3 side)
- $\boldsymbol{M_4}$: diagonal mass matrix of arms
- $\boldsymbol{M_5}$: diagonal mass matrix of forearms
- $\boldsymbol{F_v}$: diagonal matrix of viscous friction coefficients f_{vi}
- $\boldsymbol{F_c}$: diagonal matrix of Coulomb friction coefficients f_{ci}

In order to compute the dynamic modeling, some simplifications have to be done. They are listed below:

i) the weight of spatial parallelograms are represented as two ‘pinpoint’ masses at each extremity,
ii) the inertia of rods of planar parallelogram of the traveling plate is neglected,
iii) the weight of these rods is represented as two ‘pinpoint’ masses at each extremity,

B. *Modeling*

This section aims to calculate torques applied to each actuator due to several contributions. Here, the traveling plate is regarded as two separated parts, having their own contributions on torques applied to actuators.

1) Torque due to inertias

The torque due to inertias of actuators, gears and arms is defined by:

$$\boldsymbol{\tau_1} = \boldsymbol{I_{act}}\ddot{\boldsymbol{Q}} \tag{1}$$

with $I_{act} = \text{diag}\left[i_a + i_{fa} + i_m \right]$, $i_{fa} = m_5 L^2$, and diag α is a 4x4 diagonal matrix with diagonal components equal to α

2) Torque due to first half traveling plate

The contribution due to forces applied on this half traveling plate is calculated using a first jacobian matrix. This jacobian matrix $\boldsymbol{J_1}$ is calculated at point D, and is defined by the following expressions:

$$\boldsymbol{J}_1 = \boldsymbol{J}_{x1}^{-1}\boldsymbol{J}_{q1} \tag{2}$$

with

$$\boldsymbol{J}_{x1} = \begin{bmatrix} \boldsymbol{A}_0\boldsymbol{B}_0.\boldsymbol{x} & \boldsymbol{A}_0\boldsymbol{B}_0.\boldsymbol{y} & \boldsymbol{A}_0\boldsymbol{B}_0.\boldsymbol{z} & -h\cos\theta\,\boldsymbol{A}_0\boldsymbol{B}_0.\boldsymbol{x} - h\sin\theta\,\boldsymbol{A}_0\boldsymbol{B}_0.\boldsymbol{y} \\ \boldsymbol{A}_1\boldsymbol{B}_1.\boldsymbol{x} & \boldsymbol{A}_1\boldsymbol{B}_1.\boldsymbol{y} & \boldsymbol{A}_1\boldsymbol{B}_1.\boldsymbol{z} & -h\cos\theta\,\boldsymbol{A}_1\boldsymbol{B}_1.\boldsymbol{x} - h\sin\theta\,\boldsymbol{A}_1\boldsymbol{B}_1.\boldsymbol{y} \\ \boldsymbol{A}_2\boldsymbol{B}_2.\boldsymbol{x} & \boldsymbol{A}_2\boldsymbol{B}_2.\boldsymbol{y} & \boldsymbol{A}_2\boldsymbol{B}_2.\boldsymbol{z} & 0 \\ \boldsymbol{A}_3\boldsymbol{B}_3.\boldsymbol{x} & \boldsymbol{A}_3\boldsymbol{B}_3.\boldsymbol{y} & \boldsymbol{A}_3\boldsymbol{B}_3.\boldsymbol{z} & 0 \end{bmatrix} \tag{3}$$

and $$\boldsymbol{J}_{q1} = \text{diag}\left[\ \boldsymbol{A}_i\boldsymbol{B}_i \times \boldsymbol{P}_i\boldsymbol{A}_i\ .\boldsymbol{v}_i \right] \tag{4}$$

where $\cdot$ and $\times$ are respectively dot-product and cross-product.

The efforts applied to the half traveling plate are calculated using the following equation:

$$\boldsymbol{F_1} = \boldsymbol{M_1}\ \ddot{\boldsymbol{X}}_{\boldsymbol{1}} + \boldsymbol{g} \tag{5}$$

As the half traveling has only translational motions, the acceleration is calculated as follows:

$$\ddot{\boldsymbol{X}}_{\boldsymbol{1}} = \boldsymbol{T_1}\ddot{\boldsymbol{X}} \tag{6}$$

where:

$$\boldsymbol{T}_1 = \begin{bmatrix} 1 & 0 & 0 & 0 \\ 0 & 1 & 0 & 0 \\ 0 & 0 & 1 & 0 \\ 0 & 0 & 0 & 0 \end{bmatrix} \tag{7}$$

In addition,

$$\boldsymbol{M_1} = \begin{bmatrix} m_1 + m_3 + 2m_5 & 0 & 0 & 0 \\ 0 & m_1 + m_3 + 2m_5 & 0 & 0 \\ 0 & 0 & m_1 + m_3 + 2m_5 & 0 \\ 0 & 0 & 0 & I_1 \end{bmatrix} \tag{8}$$

where I_1 is the inertia of the half traveling plate. However, as this traveling plate has just translational motions, its inertia will not be useful in the modeling.

Finally, torque applied to the actuators due to the first half traveling plate is defined by:

$$\boldsymbol{\tau_2} = \boldsymbol{J_1}^T\boldsymbol{M_1}\ \ddot{\boldsymbol{X}}_{\boldsymbol{1}} + \boldsymbol{g} \tag{9}$$

3) Torque due to second half traveling plate

Forces on the second half traveling plate will produce torques on actuators. Indeed, a second Jacobean matrix $\boldsymbol{J_2}$ (calculated in D') has to be calculated.

It is defined by:

$$\boldsymbol{J}_2 = \boldsymbol{J}_{x2}^{-1}.\boldsymbol{J}_{q2} \tag{10}$$

with,

$$\boldsymbol{J}_{x2} = \begin{bmatrix} \boldsymbol{A}_0\boldsymbol{B}_0.\boldsymbol{x} & \boldsymbol{A}_0\boldsymbol{B}_0.\boldsymbol{y} & \boldsymbol{A}_0\boldsymbol{B}_0.\boldsymbol{z} & 0 \\ \boldsymbol{A}_1\boldsymbol{B}_1.\boldsymbol{x} & \boldsymbol{A}_1\boldsymbol{B}_1.\boldsymbol{y} & \boldsymbol{A}_1\boldsymbol{B}_1.\boldsymbol{z} & 0 \\ \boldsymbol{A}_2\boldsymbol{B}_2.\boldsymbol{x} & \boldsymbol{A}_2\boldsymbol{B}_2.\boldsymbol{y} & \boldsymbol{A}_2\boldsymbol{B}_2.\boldsymbol{z} & h\cos\theta.\boldsymbol{A}_2\boldsymbol{B}_2.\boldsymbol{x} + h\sin\theta.\boldsymbol{A}_2\boldsymbol{B}_2.\boldsymbol{y} \\ \boldsymbol{A}_3\boldsymbol{B}_3.\boldsymbol{x} & \boldsymbol{A}_3\boldsymbol{B}_3.\boldsymbol{y} & \boldsymbol{A}_3\boldsymbol{B}_3.\boldsymbol{z} & h\cos\theta.\boldsymbol{A}_3\boldsymbol{B}_3.\boldsymbol{x} + h\sin\theta.\boldsymbol{A}_3\boldsymbol{B}_3.\boldsymbol{y} \end{bmatrix} \tag{11}$$

and, $$\boldsymbol{J}_{q2} = \text{diag}\left[\ \boldsymbol{A}_i\boldsymbol{B}_i \times \boldsymbol{P}_i\boldsymbol{A}_i\ .\boldsymbol{v}_i \right] \tag{12}$$

The efforts applied on this second half traveling plate are defined by:

$$\boldsymbol{F}_2 = \boldsymbol{M}_2 \ \ \ddot{\boldsymbol{X}}_2 + \boldsymbol{g} \tag{13}$$

with,

$$\boldsymbol{M}_2 = \begin{bmatrix} m_2 + m_3 + 2m_5 & 0 & 0 & 0 \\ 0 & m_2 + m_3 + 2m_5 & 0 & 0 \\ 0 & 0 & m_2 + m_3 + 2m_5 & 0 \\ 0 & 0 & 0 & I_2 \end{bmatrix} \tag{14}$$

where I_2 is the inertia of the half traveling plate.

and,

$$\ddot{\boldsymbol{X}}_2 = \boldsymbol{T}_2 \ddot{\boldsymbol{X}} + \dot{\boldsymbol{T}}_2 \dot{\boldsymbol{X}} \tag{15}$$

where,

$$T_2 = \begin{bmatrix} 1 & 0 & 0 & -h\cos\theta \\ 0 & 1 & 0 & -h\sin\theta \\ 0 & 0 & 1 & 0 \\ 0 & 0 & 0 & 0 \end{bmatrix} \tag{16}$$

Finally, the torque due the second half traveling is calculated using this relation:

$$\boldsymbol{\tau}_3 = \boldsymbol{J}_2^{\ T} \boldsymbol{M}_2 \ \ \ddot{\boldsymbol{X}}_2 + \boldsymbol{g} \tag{17}$$

4) Torque due to weights of arms and forearms

This contribution is calculated using the following relation:

$$\boldsymbol{\tau_4} = -\cos \boldsymbol{Q} \ \ g\, L_G \ \ \boldsymbol{M_4} + g\, L\, \boldsymbol{M}_5 \tag{18}$$

Where L_G is the distance between P and the centre of mass of arms $\boldsymbol{P}_i\boldsymbol{A}_i$. $\cos \ \boldsymbol{Q}$ is a 4x1 vector representing the cosinus of each joint position.

5) Torque due to frictions

The torques induced by friction are calculated using the following relation:

$$\boldsymbol{\tau_5} = \boldsymbol{F_c} \operatorname{sign} \ \dot{\boldsymbol{Q}} \ + \boldsymbol{F_v} \dot{\boldsymbol{Q}} \tag{19}$$

6) Total torque

To conclude, the total torque applied to the actuators is obtained from equations (1), (9), (17), (18) and (19) corresponding to $\boldsymbol{\tau} = \sum \boldsymbol{\tau}_i$. It leads to the following equations:

$$\begin{aligned} \boldsymbol{\tau} = \boldsymbol{I_{act}} \ddot{\boldsymbol{Q}} + \boldsymbol{J_1}^T \boldsymbol{M_1} \ \ \ddot{\boldsymbol{X}}_1 + \boldsymbol{g} \ + \boldsymbol{J}_2^{\ T} \boldsymbol{M}_2 \ \ \ddot{\boldsymbol{X}}_2 + \boldsymbol{g} \\ -\cos \boldsymbol{Q} \ \ g\, L_G \ \ \boldsymbol{M_4} + g\, L\, \boldsymbol{M}_5 \ + \boldsymbol{F_c} \operatorname{sign} \ \dot{\boldsymbol{Q}} \ + \boldsymbol{F_v} \dot{\boldsymbol{Q}} \end{aligned} \tag{20}$$

C. *Validation and analysis*

The aim of the validation is to simulate the dynamics of the robot using Adams® software and to compare it with the simulation of the previous modeling, using nominal parameters. The aim is to verify that the modeling is correct, but above all to see the consequences of the simplification done at § IV.A. The robot has been completely modeled under Adams, <u>without any simplifications</u>, and a displacement has been applied. The given torques has been compared to data given by a simulation of the modeling described in this section.

Fig. 6 represents, in blue, torques obtained with Adams®; and, in red, torques given by the modeling.

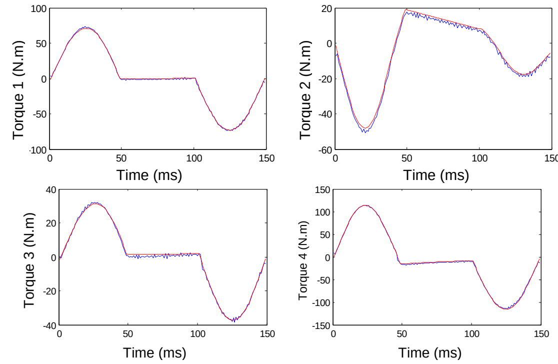

Fig. 6 Comparison of torques obtained by calculation and Adams®

This comparison shows that the simplifications have very few consequences on final results: the error between our model and Adams® is about 2%.

The final step before the implementation of the dynamic control is to perform the identification of the dynamic parameters of the robot: this is presented in the following paragraph.

V. Dynamic Identification

The dynamic modeling presented at (20) can be written in a linear form with respect to dynamic parameters. Therefore, the parameters can be estimated using a classical least square method [18].

A. *Expression of dynamic modeling*

In order to estimate the dynamic parameters, equation (20) is rewritten as follows:

$$\boldsymbol{\Gamma_{act}} = \boldsymbol{W} \boldsymbol{\chi} \tag{21}$$

where Γ_{act} is the measured torque vector, W the regressor and χ the vector of parameters to be estimated.

where

$$\boldsymbol{W} = \begin{bmatrix} \ddot{\boldsymbol{Q}} & \boldsymbol{J_1}^T \begin{bmatrix} \ddot{x}_1 \\ \ddot{y}_1 \\ \ddot{z}_1 + g \\ 0 \end{bmatrix} & \boldsymbol{J}_2^{\ T} \begin{bmatrix} \ddot{x}_2 \\ \ddot{y}_2 \\ \ddot{z}_2 + g \\ 0 \end{bmatrix} & -\cos \ \boldsymbol{Q} & \operatorname{sign} \ \dot{\boldsymbol{Q}} & \dot{\boldsymbol{Q}} \end{bmatrix} \tag{22}$$

and

$$\boldsymbol{\chi} = \begin{bmatrix} i_{act} & m'_1 & m'_2 & g & L_G m_4 + L m_5 & f_c & f_v \end{bmatrix}^T \tag{23}$$

where m'_1 and m'_2 are the sum of masses components of matrices (8) and (14).

We assume that the dynamic parameters are considered as equal for each kinematic chain. This hypothesis is done considering that all actuators are identical and the arms and the forearms are manufactured at he same time.

B. *Estimation of dynamic parameters*

Exciting trajectories are required to estimate the parameters. These trajectories are quasi-random displacements in the operational space. These motions are achieved using different phases: the first phase is a slow motion in order to highlight the friction effects, whereas the second phase is a high dynamic motion used to highlight the inertias and masses contributions.

For each trajectory performed by the robot, joint positions and voltages applied to the amplifiers are recorded. Indeed, the torque Γ_{act_i} of each actuator can be estimated using the linear relationship:

$$\Gamma_{act_i} = G_i V_i \tag{24}$$

where V_i is the voltage applied to the amplifier of motor i and G_i is its actuation gain. The gain has been obtained experimentally by measuring the force applied at the extremity of each arm for a set of voltages. This measurement had been done by pushing statically on a fixed force sensor with the end of an arm while applying different voltages to the amplifiers.

The vector of parameters $\boldsymbol{\chi}$ is estimated through a least square method applied to (22). $\boldsymbol{\Gamma}_{act}$ and $\boldsymbol{W}$ are obtained by the concatenation of 4 sets of measurement corresponding to each actuators and discretized along the exiting trajectory dunring a P closed loop motion. The calculation of the regressor $\boldsymbol{W}$ involves the calculation of joint velocities and accelerations, as well as, the computation of Cartesian acceleration. These data are calculated by the combination of a low pass filter in forward and reverse direction (Butterworth) and a derivate filter calculated by central difference. The operational acceleration is obtained by derivation of the linear kinematic relationship ($\ddot{\boldsymbol{X}} = \dot{\boldsymbol{J}}\dot{\boldsymbol{Q}} + \boldsymbol{J}\ddot{\boldsymbol{Q}}$). The results of the identification and the relative standard deviation (% σ) of each parameter are given in TABLE 1. The relative standard deviation shows that all parameters are very well estimated. Full details of this approach can be found in [18]

C. *Validation of identification*

In order to validate parameters presented in TABLE 1, a cross validation is performed. This validation consists in performing a new random trajectory. In one hand, a new set of torques applied by actuators is obtained using expression(24).

TABLE 1 ESTIMATED DYNAMIC PARAMETERS

Parameter	**Values**	**% σ**
i_{act}	0.113 kg.m^2	0.872
m'_1	0.8043 kg	0.620
m'_2	0.8594 kg	0.596
$g\ (L_G\, m_4 + L\, m_5)$	1.33 kg.m^2.s^{-2}	1.261
f_c	2.43 N.m	0.488
f_v	20.4 N.m.s.rad^{-1}	0.372

In the other hand, the torques are calculated via the dynamic modeling presented in (20), and using the parameters obtained in TABLE 1.

The results of this cross validation are given in Fig. 7 (red: the measured torques, blue: the calculated ones). This figure shows that the measured and the calculated torques are very close. This result highlights the accuracy of the estimated model.

VI. CONCLUSION

This paper has shown that Par4, a four-*dof* parallel manipulator based on the concept of articulated traveling plate is able to reach high dynamics (acceleration of 15 G). It has been explained that a dynamic model should be necessary to obtain a better dynamic accuracy. Such a model has been derived in an efficient way by resorting to only a few (and very realistic) assumptions: this model considers that the traveling plate is made of two parts and leads to the computation of two Jacobean matrices and a rather simple and compact set of equations.. This model is accurate, simple enough to be implemented in real time and has been precisely identified.

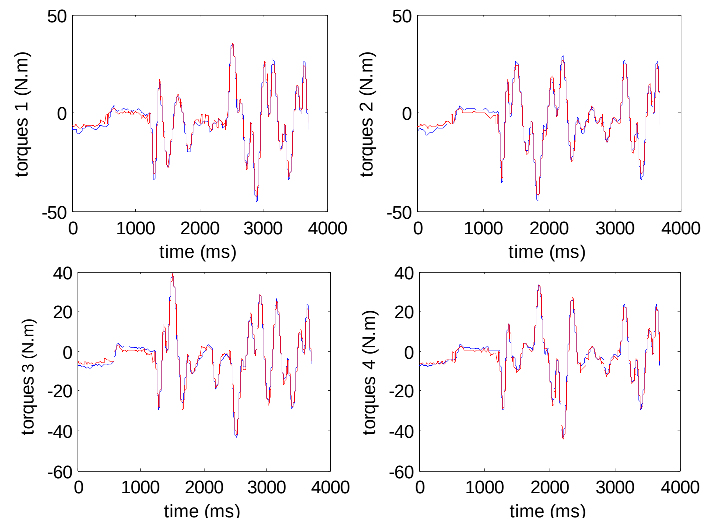

Fig. 7 Cross validation: measured and calculated torques

Our future work will be the realization of experimentations using the predictive control. The aim is to obtain a better behavior while performing very high dynamic motions, and to reach accelerations higher then 15G.

REFERENCES

[1] T. Brogardh, "PKM Research – important issues, as seen from a product development perspective at ABB robotics", in *Workshop on Fundamental Issues and Future Research Directions for Parallel Mechanisms and Manipulators*. Quebec City, Quebec, Canada: Clément M. Gosselin and Imme Erbert-Uphoff, editors, 2002.

[2] J. M. Hervé, "The lie group of rigid body displacements, a fundamental tool for mechanism design", *Mechanism and Machine Theory*, vol. 34, pp. 719-730, 1999.

[3] V. E. Gough, "Contribution to discussion of papers on research in Automotive stability, control and tyre performance", in *Proc. Auto. Div.*, Institute of mechanical engineering, 1956-1957.

[4] D. Stewart, "A platform with 6 degrees of freedom" , in *Proc. Inst. Mech. Ing.*, 1965, pp. 371-386, vol. 180, (part 1,15).

[5] R. Clavel, “Delta, a fast robot with parallel geometry”, in *18th Int.Symp. on Industrial Robots*. Lausanne: IFS Publications, april 1988, pp. 91-100.

[6] D. Chablat D, P. Wenger, " Design of a Three-Axis Isotropic Parallel Manipulator for Machining Applications: The Orthoglide ", Workshop on Fundamental Issues and Future Research Directions for Parallel Mechanisms and Manipulators, Oct.3 - 4, Québec, Canada, 2002.

[7] M. Thurneysen, M. Schnyder, R. Clavel, and J. Jiovanola, “A new parallel kinematics for high speed machine tools hita stt”, in *3rd Chemnitzer Parallelkinematik Seminar (PKS 2002)*, Chemnitz, Germany, april 23-25 2002, pp. 553ñ562.

[8] J. Angeles, A. Morozov, and O. Navarro, “A novel manipulator architecture for the production of scara motions”, in *Proceedings IEEE International Conference on Robotics and Automation*, San Francisco, USA, April 2000, pp. 2370-2375, CDROM.

[9] J. Angeles, “The Degree of Freedom of Parallel Robots: A Group-Theoretic Approach”, in *Proceedings IEEE International Conference on Robotics and Automation*, Barcelona, Spain, April 2005, pp 1017-1024, CDROM

[10] L. Rolland, “The manta and the kanuk: Novel 4-dof parallel mechanisms for industrial handling”, in *ASME Dynamic Systems and Control Division, IMECE'99 Conference*, Nashville, USA, November 1999, pp. 831-844.

[11] F. Pierrot and O. Company, “H4: a new family of 4-dof parallel Robots”, in *AIM'99: IEEE/ASME International Conference on Advanced Intelligent Mechatronics*, Atlanta, Georgia, USA, September 1999, pp. 508-513.

[12] S. Krut, V. Nabat, O. Company, and F. Pierrot, “A high speed robot for scara motions”, in *Proc. of IEEE ICRA: Int. Conf. on Robotics and Automation*, New Orleans, USA, April 26 - May 1 2004.

[13] J. M. Hervé, “The lie group of rigid body displacements, a fundamental tool for mechanism design”, *Mechanism and Machine Theory*, vol. 34, pp. 719-730, 1999.

[14] O. Company, F. Pierrot, and J. C. Fouroux, “A Method for Modeling Analytical Stiffness of a Lower Mability Parallel Manipulator’, in *Proc. Of IEEE ICRA: Int. Conf. on Robotics and Automation*, Barcelona, Spain, 18-22 April 2005.

[15] V. Nabat, O. Company, S. Krut, M. Rodriguez, F. Pierrot, “Par4: Very High Speed Parallel Robot for Pick-and-Place”, in *Proc. Of IEEE IROS: International Conference on Intelligent Robots and Systems*, Edmonton, Canada, August 2-6 2005, pp 1202-

[16] A. Vivas, P. Poignet, “Predictive Functional Control of a Parallel Robot”, in Control Engineering Practice, 2005, Vol. 13, n°7, pp. 863-874

[17] W. Khalil and O. Ibrahim, “General solution for the dynamic modeling of parallel robots”, in *Proc. of IEEE ICRA: Int. Conf. on Robotics and Automation*, New Orleans, USA, April 26 – May 1 2004

[18] A. Vivas, P. Poignet, F. Marquet, F. Pierrot and M. Gautier, “Experimental dynamic identification of a fully parallel robot”, in *Proc. of IEEE ICRA: Int. Conf. on Robotics and Automation*, Taipe, Taiwan, September 14-19, 2003